coatings

MDPI

Article

Towards Functional Silicon Nitride Coatings for Joint Replacements

Luimar Filho [1], Susann Schmidt [2,3], Klaus Leifer [1], Håkan Engqvist [1], Hans Högberg [3] and Cecilia Persson [1,*]

1 Division of Applied Materials Science, Department of Engineering Sciences, Uppsala University, Uppsala 752 37, Sweden; luimar.filho@angstrom.uu.se (L.F.); klaus.leifer@angstrom.uu.se (K.L.); hakan.engqvist@angstrom.uu.se (H.E.)
2 IHI Ionbond AG, Industriestrasse 211, Olten 4600, Switzerland; susann.schmidt@ionbond.com
3 Thin Film Physics Division, Department of Physics, Chemistry and Biology (IFM), Linköping University, Linköping 581 83, Sweden; hans.hogberg@liu.se
* Correspondence: cecilia.persson@angstrom.uu.se; Tel.: +46-184-717-911

Received: 30 November 2018; Accepted: 18 January 2019; Published: 25 January 2019

Abstract: Silicon nitride (SiN_x) coatings are currently under investigation as bearing surfaces for joint implants, due to their low wear rate and the good biocompatibility of both coatings and their potential wear debris. The aim of this study was to move further towards functional SiN_x coatings by evaluating coatings deposited onto CoCrMo surfaces with a CrN interlayer, using different bias voltages and substrate rotations. Reactive direct current magnetron sputtering was used to coat CoCrMo discs with a CrN interlayer, followed by a SiN_x top layer, which was deposited by reactive high-power impulse magnetron sputtering. The interlayer was deposited using negative bias voltages ranging between 100 and 900 V, and 1-fold or 3-fold substrate rotation. Scanning electron microscopy showed a dependence of coating morphology on substrate rotation. The N/Si ratio ranged from 1.10 to 1.25, as evaluated by X-ray photoelectron spectroscopy. Vertical scanning interferometry revealed that the coated, unpolished samples had a low average surface roughness between 16 and 33 nm. Rockwell indentations showed improved coating adhesion when a low bias voltage of 100 V was used to deposit the CrN interlayer. Wear tests performed in a reciprocating manner against Si_3N_4 balls showed specific wear rates lower than, or similar to that of CoCrMo. The study suggests that low negative bias voltages may contribute to a better performance of SiN_x coatings in terms of adhesion. The low wear rates found in the current study support further development of silicon nitride-based coatings towards clinical application.

Keywords: silicon nitride; coating; reactive high-power impulse magnetron sputtering; wear; joint replacements

1. Introduction

The need for improved materials for biomedical applications is continuously growing as a result of the increasingly active, ageing population [1–3]. Total joint replacements, such as total hip or knee replacements (THR and TKR, respectively) are commonly used in arthritic, pain-ridden patients [4], with success rates of over 90% after 10 years [1,2,5]. THRs typically consist of a ball-and-cup configuration, featuring a CoCrMo or ceramic [1] ball sliding against a polyethylene cup. Ultra-high molecular weight polyethylene (UHMWPE) has been a widely used cup material, and the recent introduction of cross-linked polyethylene (XLPE) appears to permit even lower polymer wear [6–8]. This is of great importance, since wear debris can result in inflammation, osteolysis, and loosening of the prosthesis [1,9]. Furthermore, metallic ion release and debris [10] can cause metallosis and

the formation of pseudo-tumors [11]. One possibility for reducing the metallic ion release and wear is to apply a ceramic coating on the bearing surface [12–14]. For example, TiN and ZrN coatings are currently available on the market for knee replacements, particularly aimed at hypersensitive patients [15,16]. Another possible use of ceramic coatings in joint implants is at the taper junction, which is notoriously prone to corrosion [17,18].

In this work, we investigate silicon nitride (SiN_x) coatings for joint implants. This type of coating has previously shown promising properties in terms of high biocompatibility, hardness, and low wear rates [17–20]. A further possible advantage of this coating compared to other ceramic coatings is its slow solubility in aqueous solutions [21,22], in combination with the high biocompatibility of its wear particles and ions [23]. We seek to develop SiN_x coatings that dissolve controllably and generate wear particles of a higher dissolution rate than the coating itself (due to the higher surface area), and whose dissolution also gives biocompatible ions. This, in turn, may give rise to a less negative biological response compared to other materials' wear particles. Prior work on these coatings has been focused on depositing coatings without rotation on flat, 2D substrates. As sputtering is a line-of-sight-deposition technique, the coating of 3D details such as implants requires rotation during processing. The choice of parameters for rotating the substrate table during deposition (i.e., static, 1-fold, or 3-fold substrate rotation) influences the direction (angle), the flux of sputtered material, and the energy distribution of the sputtered material arriving to the substrate [24,25]. It is necessary to control these parameters, as the properties of the sputtered material will ultimately determine the nucleation and adhesion to the substrate, as well as the initial and continued growth of the film. To secure a good adhesion between the metallic 3D substrate and the ceramic SiN_x coating, we applied growth by reactive high-power impulse magnetron sputtering (rHiPIMS), as this technique is favorable in forming a high energy flux of the sputtered material [26,27]. In addition, and for this demanding application, we applied an interlayer to promote chemical bonding in the interface region between the substrate and the coating [28].

The aim of this study was to move towards functional SiN_x coatings on 3D implants by evaluating newly developed coatings deposited onto CoCrMo with a CrN interlayer, using different bias voltages, and 1- or 3-fold rotation of the substrate. The surface roughness, coating adhesion, and chemical composition throughout the coating layers and substrate were evaluated. The coefficient of friction and wear rate against bulk Si_3N_4 were evaluated in reciprocal ball-on-disc tests.

2. Materials and Methods

2.1. Coating Preparation

Direct current magnetron sputtering processes were used to coat mirror-polished CoCrMo discs ([29], R_a < 12 nm) with a CrN interlayer, followed by a SiN_x top layer, deposited using rHiPIMS (CC800/9 ML(CemeCon AG Würselen, Germany)) in a mixed N_2 and Ar atmosphere. Substrates were mounted in a 1-fold (1f) or 3-fold (3f) rotational set-up. The specific process settings are shown in Table 1. The interlayer was deposited using a pressure of 200 MPa at negative bias voltages of 100 V (Low), 300 V (Medium), and 900 V (High). The SiN_x coatings were deposited at a pressure of 600 MPa, with an average discharge power of 3300 W using a pulse frequency of 800 Hz, and a pulse width of 200 µs in a N_2/Ar mixture with a flow ratio of 0.27.

2.2. Compositional Analysis

The chemical composition of the coatings was analyzed by X-ray photoelectron spectroscopy (XPS) (Axis UltraDLD, Kratos Analytical, Manchester, UK) using monochromatic Al (Kα) X-ray radiation ($h\nu$ = 1486.6 eV). The pressure in the analysis chamber during acquisition was less than 1×10^{-7} Pa. Samples were sputter cleaned for 120 s with a 2 keV Ar^+ ion beam. The Ar^+ beam was rastered over an area of 3×3 mm^2 at an incidence angle of 20°. Sputter cleaning was carried out to remove the surface oxygen layer and carbon due to air exposure. Automatic charge compensation was applied

throughout the acquisition, owing to the electrical insulating nature of the SiN_x coatings. The core level spectra recorded after Ar^+ sputter cleaning was used to determine the chemical composition of the SiN_x coatings, using a Shirley-type background together with elemental cross sections provided by Kratos Analytical.

2.3. Cross-Section Characterization

The coating microstructure, thickness, and composition were evaluated throughout the coating layers. A cross-section of the discs was initially sputtered by sputter coater (Au/Pd) for 30 s to reduce the charging effect, before being prepared using a focused ion beam (FIB; FEI Strata DB235, FEI, Hillsboro, OR, USA), with a platinum layer of 1 µm deposited on top to minimize the damage caused by the ion beam. The milling steps were from 7000 to 500 pA at 30 kV. Additional chemical analysis of the interlayers was undertaken using a scanning electron microscope (Zeiss Merlin with AZtec EDS/EBSD, Oberkochen, Germany) at 20 kV equipped with EDS Silicon Drift Detector AZtec (INCA energy) software (AZTEC 3.3 SP1, Oxford Instruments, High Wycombe, UK).

2.4. Surface Roughness

To evaluate the surface roughness, Vertical Scanning Interferometry (VSI), was used (WYKO NT1110, Vecco, Tucson, AZ, USA). The analyzed area was 736 × 480 μm^2 with an objective lens of 10× and Field of View (FOV) of 0.5×. Three measurements were performed on each sample. From these, the arithmetic average of the absolute values (R_a) was obtained.

2.5. Adhesion

The coating adhesion was evaluated by Rockwell indentation testing, using an applied load of 100 N with the Rockwell tip (CA1819) in three different locations according to ISO 26443-2008 [30].

2.6. Wear Resistance

Wear tests of the coatings were performed against 10 and 20 mm diameter bulk Si_3N_4 balls, manufactured according to [31]. Si_3N_4 was chosen as the counter surface to provide a worst-case scenario, hard-on-hard contact, and to simulate the coating run against itself. This facilitates a comparison with earlier work, where such a contact was used [17,19,32]. CoCrMo alloy discs, manufactured according to [33], with 21.9 mm diameter and 5 mm thickness were used as controls. The tests were performed in an in-house reciprocating ball-on-disc wear test machine, as shown in Figure 1. The applied loads were 1, 2.44, and 2.45 N, giving a maximum Hertzian contact pressure of approximately 328 MPa (20 mm ball), 442 MPa (20 mm ball), and 700 MPa (10 mm ball). The typical contact pressure in a ceramic-on-ceramic (COC) prosthesis has been estimated to 90 MPa [34]. However, in the case of edge loading by micro-separation in a ceramic-on-metal (COM) prosthesis, a contact pressure of approximately 700 MPa has been estimated, which could be considered a worst case scenario [35]. A frequency of 1 Hz and a stroke length of 10 mm was used to produce three parallel wear tracks on each sample, running for 10,000 cycles. Specimens were kept in a heated Polytetrafluoroethylene (PTFE) container with a bath at temperature of 37 ± 3 °C throughout the test. To simulate body fluid, 25 vol.% fetal bovine serum was used (FBS, GE Healthcare Hyclone, EU approved, origin South America, Chicago, IL, USA), complemented with 0.075 wt.% sodium azide (Sigma-Aldrich, St. Louis, MO, USA, S8032-25G) and 20.0 mM ethylene–diaminetetraacetic acid solution (EDTA, Sigma-Aldrich, 03690), according to [36].

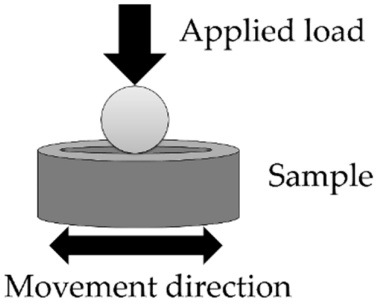

Figure 1. Schematic of the reciprocating ball-on-disc set-up for wear testing.

The specific wear rate was calculated following Archard's wear equation [37]:

$$\text{Specific wear rate} = \frac{\text{Wear volume}}{\text{Load} \times \text{sliding distance}} \quad (1)$$

where the wear volume was estimated from the cross-sectional area at the initial, middle, and final parts of the wear track, as measured with VSI after the reciprocal wear test.

2.7. Statistical Analysis

IBM SPSS Statistics v 22 was used for all statistical analyses. Welch's robust test for analysis of variance was performed (Levene's test for homogeneity of variances was significant for most analyses), followed by a Dunnett T3 post-hoc test. A critical level of $\alpha = 0.05$ was used to determine significance.

3. Results

3.1. Microstructure, Coating Thickness, and Composition

SEM cross-sections of coatings deposited using 1-fold rotation showed dense coatings (cf. Figure 2a–c), while the density, as judged upon appearance, decreased as 3-fold rotation was applied (cf. Figure 2d). The thicknesses and chemical composition of the coatings and interlayers are summarized in Table 1. A SiN_x thickness between 4.2 and 4.4 µm was measured. The coatings showed a Si content of between 43 at.% and 46 at.%, while N contents were between 50 at.% and 53 at.% and O contents of 2.1 at.%–2.2 at.% were measured, accounting for comparatively high N/Si ratios of 1.10–1.25.

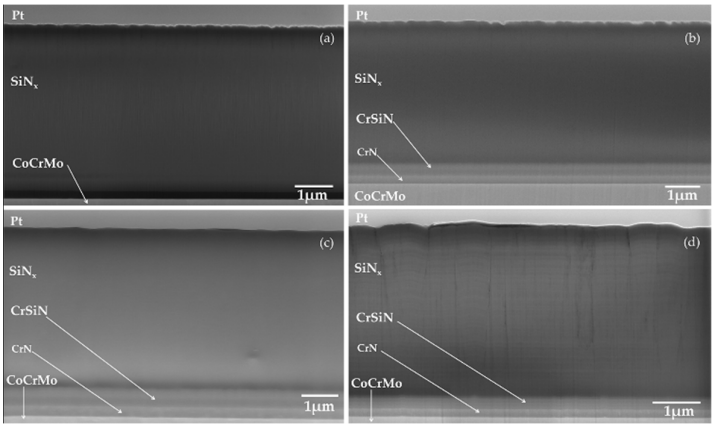

Figure 2. Cross-sections of (**a**) CoCr-SiN_x, without CrN interlayer, a dense coating could be observed; (**b**) CoCr-CrN(H)-SiN_x, deposited using 1-fold rotation and a negative bias voltage of 900 V; (**c**) CoCr-CrN(L)-SiN_x, with 1-fold rotation and a negative bias of 100 V; and (**d**) CoCr-CrN(L)-SiN_x-3f, deposited using 3-fold rotation and a negative bias of 100 V.

Table 1. The investigated materials, coating thicknesses, and chemical composition of the SiN_x top layers as measured by XPS.

Material	Interlayer	SiN_x Thickness (nm)	Interlayer Thickness (nm)	Top Layer Composition			
				Si (at.%)	N (at.%)	O (at.%)	N/Si Ratio
CoCr	–	–	–	–	–	–	–
CoCr-SiN_x	–	4360	–	46	50	2.1	1.10
CoCr-CrN(L)-SiN_x	CrN	4260	810	44	52	2.2	1.11
CoCr-CrN(M)-SiN_x	CrN	4400	750	44	53	2.1	1.19
CoCr-CrN(H)-SiN_x	CrN	4400	650	43	53	2.2	1.25
CoCr-CrN(L)-SiN_x-3f	CrN	4200	500	45	51	–	1.11

3.2. Surface Roughness

According to the standard for biomedical implants [38], the average surface roughness (R_a) of bearing surfaces or femoral heads of metallic or ceramic surfaces must be below 50 nm. Both coated and uncoated samples exhibited a surface roughness below this requirement (16–33 nm and 7 nm, respectively). As reported in Table 2, the roughness of the uncoated CoCrMo surface was significantly lower than that of the coated surfaces ($\alpha < 0.05$). The coating without an interlayer was significantly smoother (R_a = 16.3 nm) than the coatings deposited with an interlayer bias voltage (100, 300, and 900 V, $\alpha < 0.02$, R_a ranging between 23.9 and 32.8 nm). No significant difference in R_a was observed for coatings deposited at the low bias voltage (L) in either 1f or 3f rotations ($\alpha > 0.05$, R_a = 25.2 and 23.9 nm on average, respectively).

Table 2. Surface roughness and adhesion of the investigated materials.

Material	R_a (nm)	HRC Adhesion, (ISO Class)
CoCr	6.6 ± 0.4	N/A
CoCr-SiN_x	16.3 ± 1.8	3
CoCr-CrN(L)-SiN_x	25.2 ± 0.1	1
CoCr-CrN(M)-SiN_x	26.1 ± 1.2	2
CoCr-CrN(H)-SiN_x	32.8 ± 2.7	2
CoCr-CrN(L)-SiN_x-3f	23.9 ± 0.7	0–1

3.3. Adhesion

Results for the Rockwell C (HRC) adhesion tests are presented in Table 2. Improved values for coatings featuring a CrN interlayer were found compared to those without. Furthermore, a lower bias voltage during the CrN interlayer formation appeared to benefit the adhesion. For coatings deposited under 3-fold rotation, the adhesion improved further, to an HRC ISO class 0–1.

3.4. Wear Resistance

The initial stage of the experiment showed a higher friction coefficient (0.78 and 0.48 at 700 MPa, 0.51 and 0.39 at 442 MPa, and 0.48 and 0.33 at 328 MPa) for coated and non-coated samples respectively, which stabilized after 2000 cycles. The coefficient of friction was therefore averaged after the running-in phase, i.e., for the cycles between 2000 and 10,000, and is reported in Figure 3. The friction coefficients against the coatings were slightly higher than those against CoCr. However, a statistically significant difference was only found between CoCr and CoCr-CrN(H)-SiN_x (α = 0.04 at the 328 MPa contact pressure).

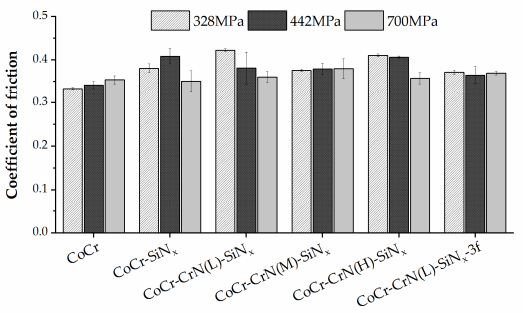

Figure 3. Coefficient of friction at estimated contact pressures of 328 and 442 MPa, using a ball diameter of 20 mm, with applied loads of 1 and 2.45 N, respectively. The coefficient of friction at an estimated contact pressure of 700 MPa is also included, using a ball diameter of 10 mm and an applied load of 2.44 N.

For the ball of diameter 20 mm, CoCr showed a higher specific wear rate compared to coated samples at the lower contact pressure of 328 MPa, but a similar wear rate at the higher contact pressure of 442 MPa. For the 442 MPa contact pressure, a significant difference could be found only between CoCr-SiN_x and CoCr-CrN(L)-SiN_x-3f ($\alpha = 0.015$), with the latter giving the lowest specific wear rate of all samples. For the smaller ball diameter (10 mm), CoCr again showed a higher wear rate than the coated samples, as shown in Figure 4. All wear tracks were analyzed by VSI and reported on Figure A1.

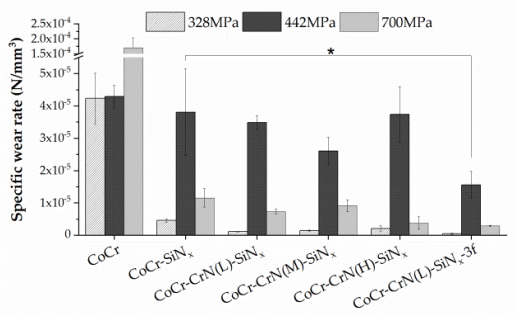

Figure 4. Specific wear rates at 328 and 442 MPa, ran against a 20 mm Si_3N_4 ball, as well as at 700 MPa with 10 mm ball. * Statistically significant difference.

4. Discussion

This study evaluated the effects of: (i) The addition of a CrN interlayer prior to depositing the SiN_x coating; (ii) different bias voltages during interlayer formation; and (iii) the level of rotation during deposition on coating properties and wear performance.

Coatings deposited by 1f rotation presented uniform, featureless, and dense structures, while coatings deposited in a 3-fold rotation set-up showed a comparatively facetted growth with visible columns, as illustrated in Figure 2. This is related to the arrival rate of film-forming species as well as their energy during coating growth, where samples mounted in the 1f rotational set-up are exposed to more and higher energetic film forming species per time unit [39–41].

The coatings showed a high N content, with N/Si ratios between 1.10 and 1.25. In earlier studies, this has been found to be beneficial, in terms of a lower dissolution rate [21] and improved mechanical properties [42].

The average surface roughness of the coatings as deposited ranged between 16 and 23 nm, fulfilling the standard requirements for joint bearing surfaces, although post-polishing would likely be employed for commercial purposes. These higher roughness values as compared to the non-coated surface indicate the existence of coating facets, as shown in Figure 2. Other coatings for joint implants

deposited using rHiPIMS (but using different deposition parameters) have shown similar roughness values [26,28].

The coating adhesion was improved by the implementation of a CrN interlayer, and was better for the 3-fold coatings compared to the 1-f coatings, with the latter result likely arising from a lower coating density giving lower residual stresses, as a result of the increased rotation [25]. The enhancement in adhesion after CrN addition was comparable to previous work [43,44].

The coefficient of friction of 0.33–0.42 is in the range of those reported in earlier, comparable wear studies on ceramic-on-ceramic implants (0.25–0.8) [45], but in the higher range of our earlier studies on SiN_x coatings [17,32]. The specific wear rates were also higher in general, except for CoCr at 328 MPa and 442 MPa [17,32]. These differences may be due to differences in coating morphology and density, counter surface ball sizes, and, in some cases, higher loads applied in the current study [46]. Other experimental coatings for joint implants have shown specific wear rates in the same order of magnitude under similar tests conditions. However direct comparisons are difficult due to variations in the set-up [17,32,47–49]. Formation of a tribofilm between the surfaces may occur during wear tests of these materials, resulting in a lubrication effect that reduces the wear and the coefficient of friction [50–52]. However, this was not investigated herein.

Wear rates at the lowest load show promising results for both ball sizes, while coating wear rates approached those of CoCr for the higher load (larger ball size). The highest contact pressure was chosen based on simulated micro separation studies for COC contacts [53]. Even higher contact pressures of around 1 GPa have, however, been reported in other studies for edge loading conditions [35]. Therefore, for hard-on-hard contacts, further testing should be considered at higher contact pressures. However, it should be noted that these cases are to be considered as worst-case scenarios. In fact, most joint prostheses currently implanted use a hard-on-soft bearing, i.e., a metal or ceramic actuating against a polymer. Therefore, further testing against polymeric surfaces would be of high interest. In addition, tests performed in a setting more similar to that of the end application, such as in joint simulators, and for longer periods of time, are needed.

5. Conclusions

SiN_x coatings were deposited onto CoCrMo substrates by rHiPIMS, under 1- and 3-fold rotation, to evaluate the resulting properties for possible application in joint implants. It could be concluded that:

- 3-fold deposition gave rise to less dense coatings as compared to 1-fold rotation, as demonstrated by the FIB cross-sections;
- The deposition method resulted in wear-resistant coatings, with no wearing down or flaking off when run against Si_3N_4, likely due to their high N content as well as their relatively high density;
- Despite the relatively higher roughness and lower density, the CoCr-CrN(L)-SiN_x-3f coating, deposited at a lower bias voltage and by 3-fold rotation, presented the lowest specific wear rate against Si_3N_4 balls, also compared to a CoCrMo control.

The present results indicate some promising properties of these coatings, although further studies are needed, especially in a 3D setting on full hip implants.

Author Contributions: Conceptualization, S.S., H.E., H.H. and C.P.; Methodology, L.F., S.S. and C.P.; Validation, L.F. and S.S.; Formal Analysis, L.F., S.S. and C.P.; Investigation, L.F. and S.S.; Resources, C.P., H.H., K.L. and H.E.; Writing—Original Draft Preparation, L.F., S.S. and C.P.; Writing—Review and Editing, L.F., S.S., K.L., H.E., H.H. and C.P.; Visualization, L.F., S.S. and C.P.; Supervision, K.L., H.E., H.H. and C.P.; Project Administration, H.H., H.E. and C.P.; Funding Acquisition, C.P., H.E., H.H. and K.L.

Funding: This research was funded by the European Union, No. FP7-NMP-2012-310477 (Life Long Joints project); the Erasmus Mundus Programme, Euro-Brazilian Windows + Project, No. 2014-0982; the Swedish Government Strategic Research Area in Materials Science on Advanced Functional Materials, No. 2009-00971.

Acknowledgments: Susan Peacock is gratefully acknowledged for proof-reading.

Conflicts of Interest: Håkan Engqvist is co-inventor on a patent related to similar coatings.

Appendix A

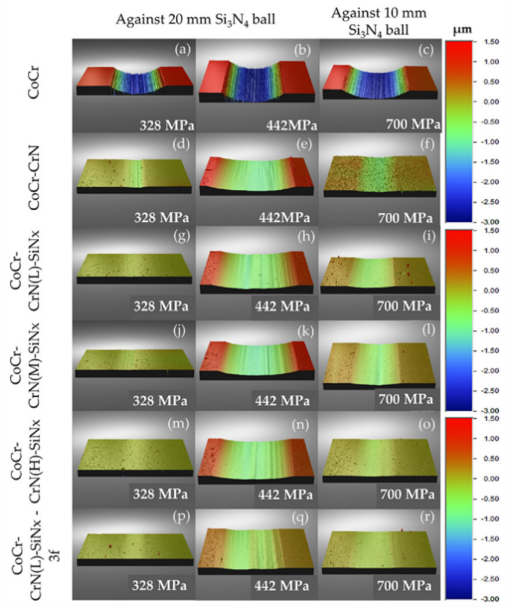

Figure A1. Typical wear tracks from reciprocal wear tests against Si_3N_4, as analyzed by Vertical Scanning Interferometry (VSI).

References

1. Kärrholm, J.; Lindahl, H.; Malchau, H.; Mohaddes, M.; Rogmark, C.; Rolfson, O. *Swedish Hip Arthroplasty Register Annual Report 2015*; Swedish Hip Arthroplasty Register: Gothenburg, Sweden, 2015.
2. Sundberg, M.; Lidgren, L.; W-Dahl, A.; Robertsson, O. *Swedish Knee Arthroplasty Register Annual Report 2015*; Swedish Hip Arthroplasty Register: Lund, Sweden, 2015.
3. Verheyen, C.C.; Verhaar, J.A. Failure rates of stemmed metal-on-metal hip replacements. *Lancet* **2012**, *380*, 105. [CrossRef]
4. Learmonth, I.D.; Young, C.; Rorabeck, C. The operation of the century: Total hip replacement. *Lancet* **2007**, *370*, 1508–1519. [CrossRef]
5. Pettersson, M. Silicon Nitride for Total Hip Replacements. Ph.D. Thesis, Uppsala University, Uppsala, Sweden, May 2015.
6. Berry, D.J.; Abdel, M.P.; Callaghan, J.J. What are the current clinical issues in wear and tribocorrosion? *Clin. Orthop. Relat. Res.* **2014**, *472*, 3659–3664. [CrossRef] [PubMed]
7. Kurtz, S.M.; Medel, F.J.; MacDonald, D.W.; Parvizi, J.; Kraay, M.J.; Rimnac, C.M. Reasons for revision of first-generation highly cross-linked polyethylenes. *J. Arthroplast.* **2010**, *25*, 67–74. [CrossRef] [PubMed]
8. Kurtz, S.M.; Gawel, H.A.; Patel, J.D. History and systematic review of wear and osteolysis outcomes for first-generation highly crosslinked polyethylene. *Clin. Orthop. Relat. Res.* **2011**, *469*, 2262–2277. [CrossRef] [PubMed]
9. Lee, J.; Salvati, E.; Betts, F.; DiCarlo, E.; Doty, S.; Bullough, P. Size of metallic and polyethylene debris particles in failed cemented total hip replacements. *J. Bone Jt. Surg. Br. Vol.* **1992**, *74*, 380–384. [CrossRef]
10. Drummond, J.; Tran, P.; Fary, C. Metal-on-metal hip arthroplasty: A review of adverse reactions and patient management. *J. Funct. Biomater.* **2015**, *6*, 486–499. [CrossRef]
11. Bitounis, D.; Pourchez, J.; Forest, V.; Boudard, D.; Cottier, M.; Klein, J.P. Detection and analysis of nanoparticles in patients: A critical review of the status quo of clinical nanotoxicology. *Biomaterials* **2016**, *76*, 302–312. [CrossRef]
12. Ayu, H.M.; Izman, S.; Daud, R.; Krishnamurithy, G.; Shah, A.; Tomadi, S.H.; Salwani, M.S. Surface modification on CoCrMo alloy to improve the adhesion strength of hydroxyapatite coating. *Procedia Eng.* **2017**, *184*, 399–408. [CrossRef]
13. Datta, S.; Das, M.; Krishna, V.; Bodhak, S.; Murugesan, V.K. Mechanical, wear, corrosion and biological properties of arc deposited titanium nitride coatings. *Surf. Coat. Technol.* **2018**, *344*, 214–222. [CrossRef]

14. Marchiori, G.; Lopomo, N.; Boi, M.; Berni, M.; Bianchi, M.; Gambardella, A.; Visani, A.; Russo, A.; Marcacci, M. Optimizing thickness of ceramic coatings on plastic components for orthopedic applications: A finite element analysis. *Mater. Sci. Eng. C* **2016**, *58*, 381–388. [CrossRef] [PubMed]
15. Grupp, T.M.; Giurea, A.; Miehlke, R.K.; Hintner, M.; Gaisser, M.; Schilling, C.; Schwiesau, J.; Kaddick, C. Biotribology of a new bearing material combination in a rotating hinge knee articulation. *Acta Biomater.* **2013**, *9*, 7054–7063. [CrossRef] [PubMed]
16. Ajwani, S.H.; Charalambous, C.P. Availability of total knee arthroplasty implants for metal hypersensitivity patients. *Knee Surg. Relat. Res.* **2016**, *28*, 312–318. [CrossRef] [PubMed]
17. Pettersson, M.; Tkachenko, S.; Schmidt, S.; Berlind, T.; Jacobson, S.; Hultman, L.; Engqvist, H.; Persson, C. Mechanical and tribological behavior of silicon nitride and silicon carbon nitride coatings for total joint replacements. *J. Mech. Behav. Biomed. Mater.* **2013**, *25*, 41–47. [CrossRef] [PubMed]
18. Mazzocchi, M.; Bellosi, A. On the possibility of silicon nitride as a ceramic for structural orthopaedic implants. Part I: Processing, microstructure, mechanical properties, cytotoxicity. *J. Mater. Sci. Mater. Med.* **2008**, *19*, 2881–2887. [CrossRef] [PubMed]
19. Bal, B.S.; Khandkar, A.; Lakshminarayanan, R.; Clarke, I.; Hoffman, A.A.; Rahaman, M.N. Fabrication and testing of silicon nitride bearings in total hip arthroplasty: Winner of the 2007 "HAP" PAUL award. *J. Arthroplast.* **2009**, *24*, 110–116. [CrossRef] [PubMed]
20. Rahaman, M.; Xiao, W. Silicon nitride bioceramics in healthcare. *Int. J. Appl. Ceram. Technol.* **2018**, *15*, 861–872. [CrossRef]
21. Pettersson, M.; Bryant, M.; Schmidt, S.; Engqvist, H.; Hall, R.M.; Neville, A.; Persson, C. Dissolution behaviour of silicon nitride coatings for joint replacements. *Mater. Sci. Eng. C* **2016**, *62*, 497–505. [CrossRef]
22. Pettersson, M.; Skjöldebrand, C.; Filho, L.; Engqvist, H.; Persson, C. Morphology and dissolution rate of wear debris from silicon nitride coatings. *ACS Biomater. Sci. Eng.* **2016**, *2*, 998–1004. [CrossRef]
23. Lal, S.; Hall, R.M.; Tipper, J.L. A novel method for isolation and recovery of ceramic nanoparticles and metal wear debris from serum lubricants at ultra-low wear rates. *Acta Biomater.* **2016**, *42*, 420–428. [CrossRef]
24. Hovsepian, P.E.; Ehiasarian, A.P.; Purandare, Y.P.; Biswas, B.; Pérez, F.J.; Lasanta, M.I.; De Miguel, M.T.; Illana, A.; Juez-Lorenzo, M.; Muelas, R.; et al. Performance of HIPIMS deposited CrN/NbN nanostructured coatings exposed to 650 °C in pure steam environment. *Mater. Chem. Phys.* **2016**, *179*, 110–119. [CrossRef]
25. Paulitsch, J.; Schenkel, M.; Zufraß, T.; Mayrhofer, P.H.; Münz, W.D. Structure and properties of high power impulse magnetron sputtering and DC magnetron sputtering CrN and TiN films deposited in an industrial scale unit. *Thin Solid Films* **2010**, *518*, 5558–5564. [CrossRef]
26. Ma, Q.; Li, L.; Xu, Y.; Gu, J.; Wang, L.; Xu, Y. Effect of bias voltage on TiAlSiN nanocomposite coatings deposited by HiPIMS. *Appl. Surf. Sci.* **2017**, *392*, 826–833. [CrossRef]
27. Bohlmark, J.; Lattemann, M.; Gudmundsson, J.T.; Ehiasarian, A.P.; Aranda Gonzalvo, Y.; Brenning, N.; Helmersson, U. The ion energy distributions and ion flux composition from a high power impulse magnetron sputtering discharge. *Thin Solid Films* **2006**, *515*, 1522–1526. [CrossRef]
28. Williams, S.; Isaac, G.; Hatto, P.; Stone, M.H.; Ingham, E.; Fisher, J. Comparative wear under different conditions of surface-engineered metal-on-metal bearings for total hip arthroplasty. *J. Arthroplast.* **2004**, *19*, 112–117. [CrossRef]
29. *ASTM F799-11 Standard Specification for Cobalt-28Chromium-6Molybdenum Alloy Forgings for Surgical Implants (UNS R31537, R31538, R31539)*; ASTM International: West Conshohocken, PA, USA, 2011.
30. *ISO 26443-2008 Fine Ceramics (Advanced Ceramics, Advanced Technical Ceramics) Rockwell Indentation Test for Evaluation of Adhesion of Ceramic Coatings*; ISO: Geneva, Switzerland, 2008.
31. *ASTM F2094/F2094M-18a Standard Specification for Silicon Nitride Bearing Balls*; ASTM International: West Conshohocken, PA, USA, 2018.
32. Olofsson, J.; Pettersson, M.; Teuscher, N.; Heilmann, A.; Larsson, K.; Grandfield, K.; Persson, C.; Jacobson, S.; Engqvist, H. Fabrication and evaluation of Si_xN_y coatings for total joint replacements. *J. Mater. Sci. Mater. Med.* **2012**, *23*, 1879–1889. [CrossRef] [PubMed]
33. *ASTM F1537-11 Standard Specification for Wrought Cobalt-28Chromium-6Molybdenum Alloys for Surgical Implants (UNS R31537, UNS R31538, and UNS R31539)*; ASTM International: West Conshohocken, PA, USA, 2011.
34. Fialho, J.C.; Fernandes, P.R.; Eça, L.; Folgado, J. Computational hip joint simulator for wear and heat generation. *J. Biomech.* **2007**, *40*, 2358–2366. [CrossRef]

35. Sanders, A.P.; Brannon, R.M. Assessment of the applicability of the Hertzian contact theory to edge-loaded prosthetic hip bearings. *J. Biomech.* **2011**, *44*, 2802–2808. [CrossRef]
36. *ASTM F732-17 Standard Test Method for Wear Testing of Polymeric Materials Used in Total Joint Prostheses*; ASTM International: West Conshohocken, PA, USA, 2017.
37. Archard, J.F. Contact and rubbing of flat surfaces. *J. Appl. Phys.* **1953**, *24*, 981–988. [CrossRef]
38. *ASTM F2033-12 Standard Specification for Total Hip Joint Prosthesis and Hip Endoprosthesis Bearing Surfaces Made of Metallic, Ceramic, and Polymeric Materials*; ASTM International: West Conshohocken, PA, USA, 2012.
39. Nedfors, N.; Mockute, A.; Palisaitis, J.; Persson, P.O.Å.; Näslund, L.Å.; Rosen, J. Influence of pulse frequency and bias on microstructure and mechanical properties of TiB_2 coatings deposited by high power impulse magnetron sputtering. *Surf. Coat. Technol.* **2016**, *304*, 203–210. [CrossRef]
40. Panjan, M.; Čekada, M.; Panjan, P.; Zupanič, F.; Kölker, W. Dependence of microstructure and hardness of TiAlN/VN hard coatings on the type of substrate rotation. *Vacuum* **2012**, *86*, 699–702. [CrossRef]
41. Ehiasarian, A.P.; Münz, W.D.; Hultman, L.; Helmersson, U.; Petrov, I.; Seitz, F. High power pulsed magnetron sputtered CrN_x films. *Galvanotechnik* **2003**, *163*, 267–272. [CrossRef]
42. Schmidt, S.; Hänninen, T.; Goyenola, C.; Wissting, J.; Jensen, J.; Hultman, L.; Goebbels, N.; Tobler, M.; Högberg, H. SiN_x coatings deposited by reactive high power impulse magnetron sputtering: Process parameters influencing the nitrogen content. *ACS Appl. Mater. Interfaces* **2016**, *8*, 20385–20395. [CrossRef] [PubMed]
43. Ortega-Saenz, J.A.; Hernandez-Rodriguez, M.A.L.; Ventura-Sobrevilla, V.; Michalczewski, R.; Smolik, J.; Szczerek, M. Tribological and corrosion testing of surface engineered surgical grade CoCrMo alloy. *Wear* **2011**, *271*, 2125–2131. [CrossRef]
44. Sahasrabudhe, H.; Bose, S.; Bandyopadhyay, A. Laser processed calcium phosphate reinforced CoCrMo for load-bearing applications: Processing and wear induced damage evaluation. *Acta Biomater.* **2018**, *66*, 118–128. [CrossRef]
45. Dante, R.C.; Kajdas, C.K. A review and a fundamental theory of silicon nitride tribochemistry. *Wear* **2012**, *288*, 27–38. [CrossRef]
46. López, A.; Filho, L.C.; Cogrel, M.; Engqvist, H.; Schmidt, S.; Högberg, H.; Persson, C. Morphology and adhesion of silicon nitride coatings upon soaking in fetal bovine serum. In Proceedings of the 15th International Symposium on Computer Methods in Biomechanics and Biomedical Engineering and the 3rd Conference on Imaging and Visualization, Lisbon, Portugal, 26–29 March 2018.
47. Saikko, V.; Calonius, O.; Kernen, J. Effect of counterface roughness on the wear of conventional and crosslinked ultrahigh molecular weight polyethylene studied with a multi-directional motion pin-on-disk device. *J. Biomed. Mater. Res.* **2001**, *57*, 506–512. [CrossRef]
48. Williams, S.; Tipper, J.L.; Ingham, E.; Stone, M.H.; Fisher, J. In vitro analysis of the wear, wear debris and biological activity of surface-engineered coatings for use in metal-on-metal total hip replacements. *Proc. Inst. Mech. Eng. Part H J. Eng. Med.* **2003**, *217*, 155–163. [CrossRef]
49. Leslie, I.J.; Williams, S.; Brown, C.; Anderson, J.; Isaac, G.; Hatto, P.; Ingham, E.; Fisher, J. Surface engineering: A low wearing solution for metal-on-metal hip surface replacements. *J. Biomed. Mater. Res. Part B Appl. Biomater.* **2009**, *90*, 558–565. [CrossRef]
50. Bal, B.S.; Rahaman, M.N. Orthopedic applications of silicon nitride ceramics. *Acta Biomater.* **2012**, *8*, 2889–2898. [CrossRef]
51. Olofsson, J.; Grehk, T.M.; Berlind, T.; Persson, C.; Jacobson, S.; Engqvist, H. Evaluation of silicon nitride as a wear resistant and resorbable alternative for total hip joint replacement. *Biomatter* **2012**, *2*, 94–102. [CrossRef] [PubMed]
52. Das, M.; Bhimani, K.; Balla, V.K. In vitro tribological and biocompatibility evaluation of sintered silicon nitride. *Mater. Lett.* **2018**, *212*, 130–133. [CrossRef]
53. Mak, M.; Jin, Z.; Fisher, J.; Stewart, T.D. Influence of acetabular cup rim design on the contact stress during edge loading in ceramic-on-ceramic hip prostheses. *J. Arthroplast.* **2011**, *26*, 131–136. [CrossRef] [PubMed]